Supplementary Data

Green and sustainable zero-waste conversion of water hyacinth (*Eichhornia crassipes*) into superior magnetic carbon composite and supercapacitor electrodes

Amonrada Saning[a], Servann Herou[b], Decha Dechtrirat[c], Chanoknan Ieosakulrat[d], Pasit Pakawatpanurut[d], Sulawan Kaowphong[e], Chanchana Thanachayanont[f], Maria-Magdalena Titirici[b,g], Laemthong Chuenchom[a]*

[a]*Department of Chemistry and Center for Excellence for Innovation in Chemistry (PERCH-CIC), Faculty of Science, Prince of Songkla University, Hat-Yai, Songkhla 90112, Thailand.*

[b]*Imperial College London, Department of Chemical Engineering, South Kensington Campus, SW7 2AZ, United Kingdom*

[c]*Department of Materials Science, Faculty of Science, Kasetsart University, Ngam Wong Wan Road, Lat Yao Chatuchak Bangkok 10900, Thailand*

[d]*Department of Chemistry and Center of Excellence for Innovation in Chemistry (PERCH-CIC), Faculty of Science, Mahidol University, Rama VI Rd, Bangkok 10400, Thailand.*

[e]*Department of Chemistry, Faculty of Science, Chiang Mai University, Chiang Mai 50200, Thailand.*

[f]*National Metal and Materials Technology Center (MTEC), National Science and Technology Development Agency (NSTDA), Pathumthani 12120, Thailand*

[g]*Queen Mary University of London, School of Engineering and Materials Science, Mile End Road, E1 4NS, London, UK*

* Corresponding author. Tel.: +66 74 288416; fax: +66 74 558841.

Email address: laemthong.c@psu.ac.th (L. Chuenchom)

T-Cell scheme

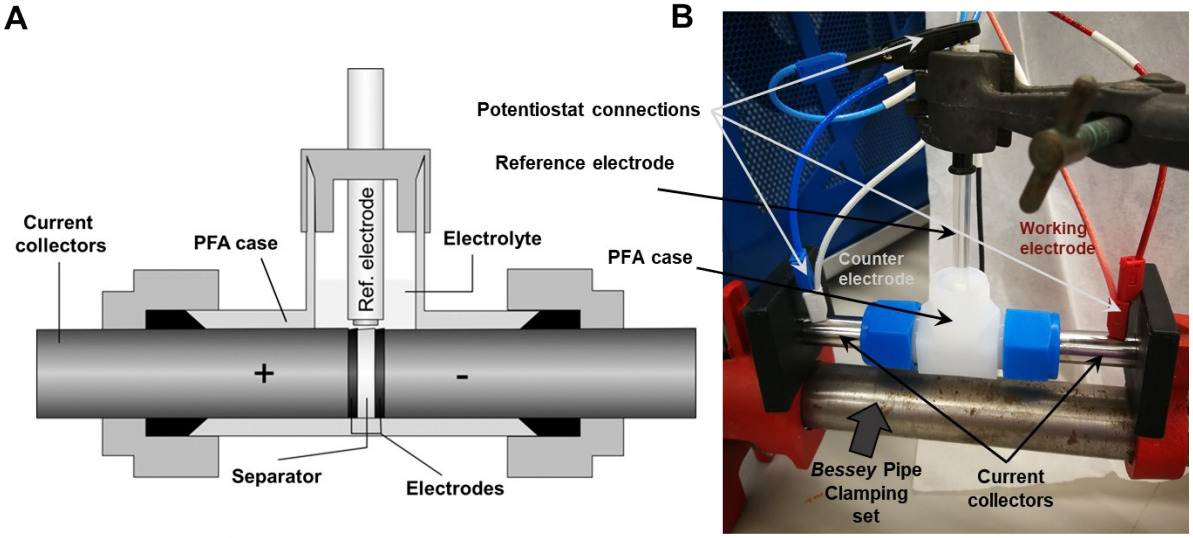

Fig. S1 (a) Section of a Swagelok cell (taken from M. Karthik et al [1]) (b) Picture of the electrochemical cell.

Electrolyte stability – Voltage window

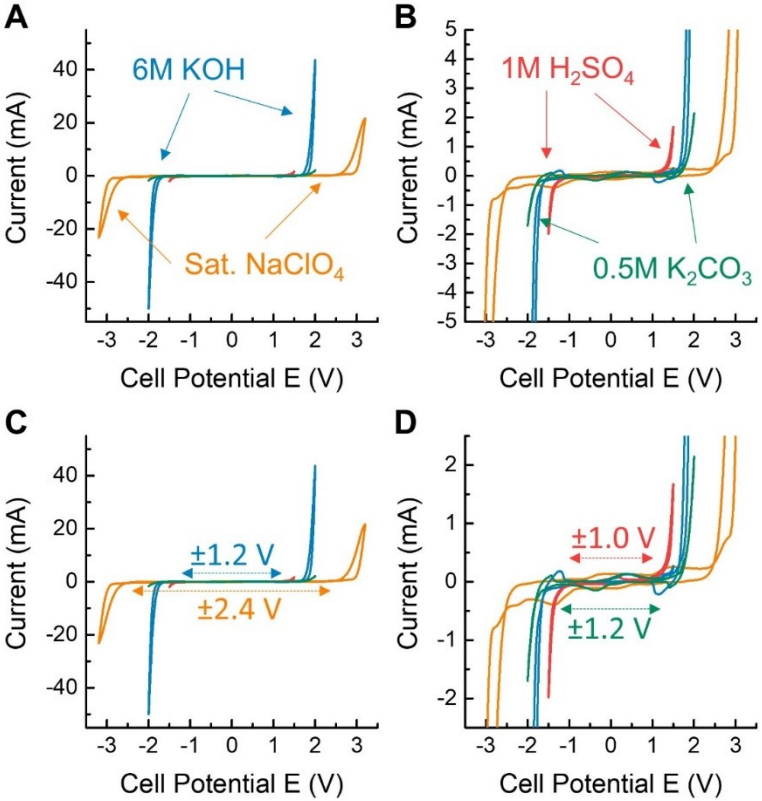

Fig. S2 Electrochemical stability window of 6MKOH compared to other electrolytes (1M H_2SO_4, 0.5M K_2CO_3 and saturated $NaClO_4$). (a) and (b), Cyclovoltammograms showing the corrosion or degradation current peaks observed at various potentials; (c) and (d) Cyclovoltammograms showing the stable electrochemical potential window chosen for each electrolyte. It is seen that 6M KOH allows a voltage window of 1.2 V while avoiding electrolyte degradation at high overpotential.

Table S1. Elemental compositions of prepared carbon materials characterized by XPS.

Materials	wt%						
	C	**O**	**N**	**Ca**	**Si**	**Mg**	**Cl**
MWHHTC	65.80	27.63	1.84	2.75	1.95	-	-
MWHHTC(1)-800	76.45	16.44	-	7.10	-	-	-
CLP	60.82	24.60	4.73	2.93	1.34	2.59	2.98
CLP+KOH-800	78.73	15.05	-	-	6.22	-	-

Table S2. %Area of functional groups derived from C1s deconvolution XPS spectra of prepared materials.

Materials	%Area					
	C=C	C-O	C-O-C	C=O	O-C=O	π–π^*
MWHHTC	43.3	14.0	22.2	14.0	6.4	-
MWHHTC(1)-800	65.5	16.7	6.8	4.6	4.0	2.4
CLP	43.3	14.0	22.2	14.0	-	-
CLP+KOH-800	64.9	16.6	8.4	5.2	5.0	-

Table S3. BET surface area, total pore volume micropore volume and mesopore fraction of prepared materials.

Materials	BET surface area (m^2 g^{-1})	total pore volume (cm^3 g^{-1})	micropore volume (cm^3 g^{-1})	mesopore fraction (%)
MWHHTC	7.35	0.0440	0.0006	98.64
MWHHTC(1)-800	973.56	0.6217	0.0888	85.71
CLP-800	144.70	0.0849	0.0311	62.64
CLP+KOH-800	2544.87	1.4563	0.0889	93.90

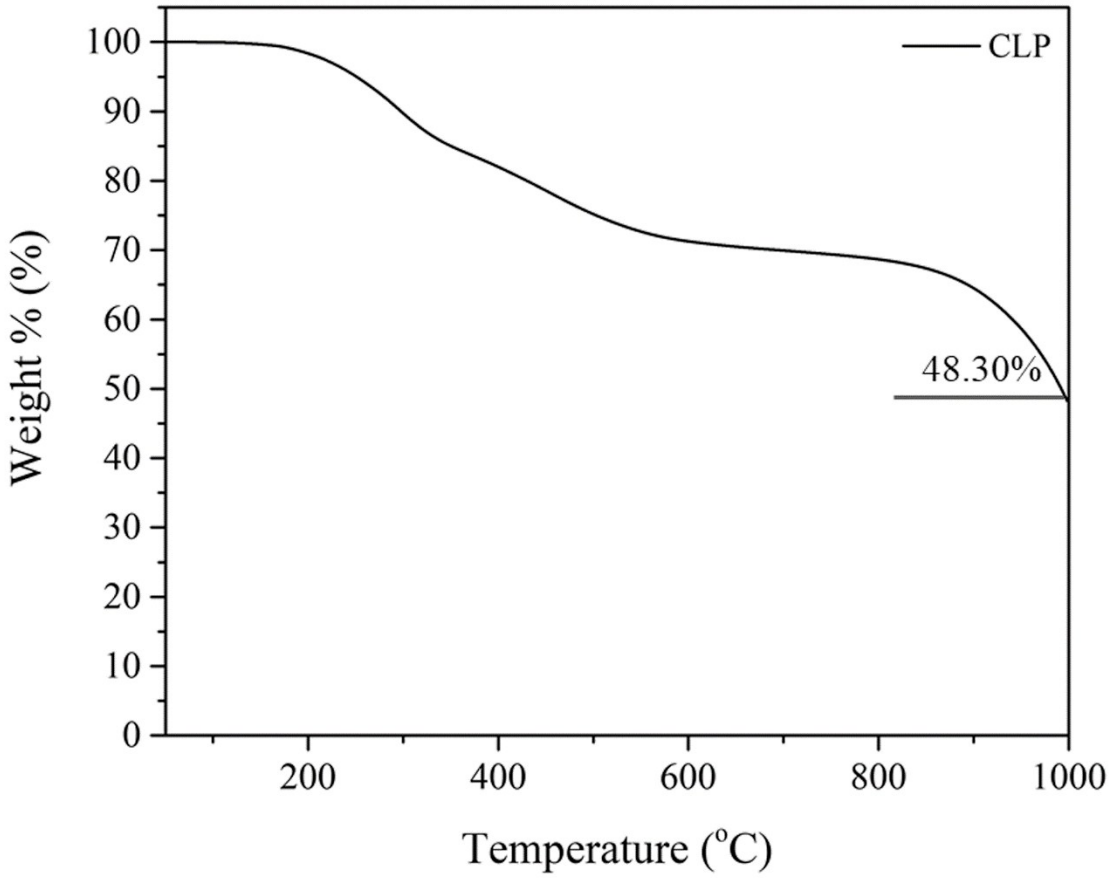

Fig. S3. TGA thermogram of CLP. The experiment was performed from 50-1000 °C (ramp rate: 10 °C min^{-1})

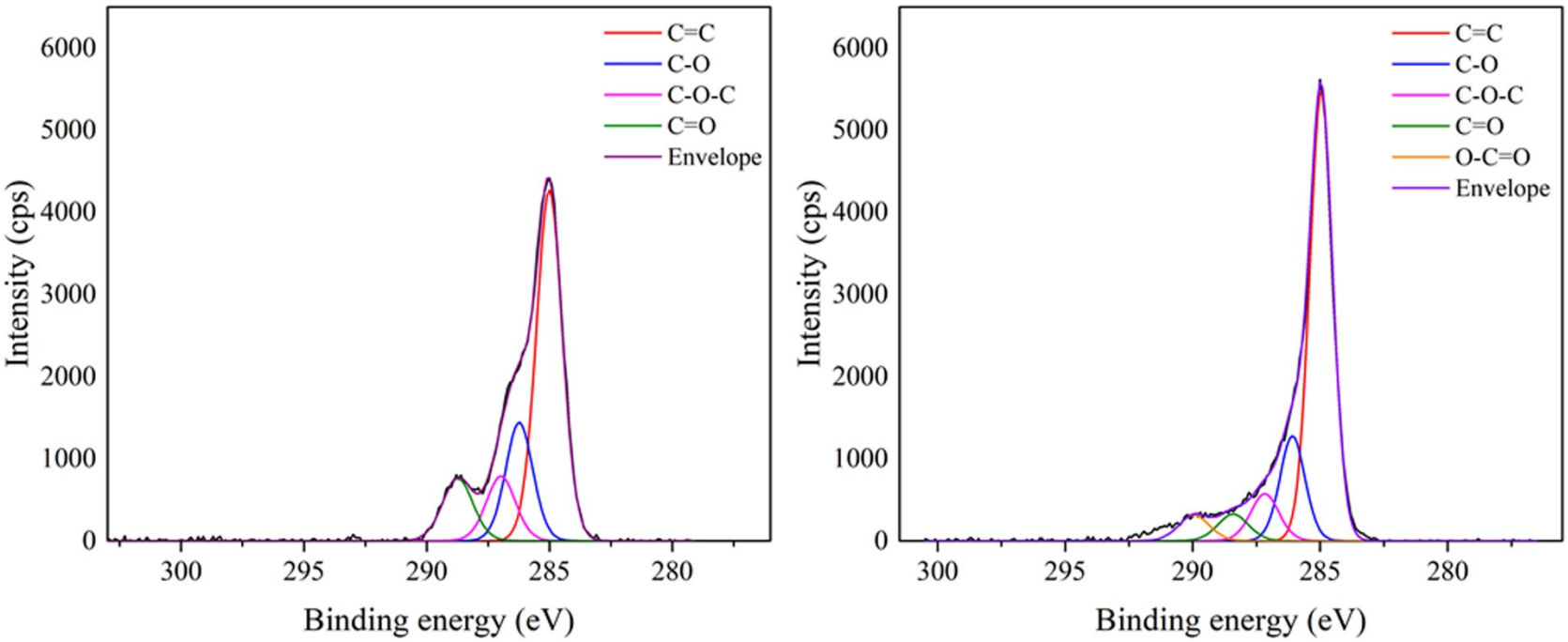

Fig. S4. XPS C1s spectra of (a) WHHTC and (b) MWHHTC(1)-800.

Table S4. Pseudo second kinetic and Langmuir parameters of MWHHTC(1)-800 on MB, MO and TC adsorption.

Adsorbate	Pseudo second kinetic model			Langmuir model		
	k_2 (g (mg min)$^{-1}$)	q_e (mg g^{-1})	R^2	K_L(L mg^{-1})	q_{max} (mg g^{-1})	R^2
Methylene blue	9.14×10^{-5}	500.41	0.99806	5.6447	524.20	0.90041
Methyl orange	2.73×10^{-4}	421.61	0.99913	1.1772	425.15	0.99781
Tetracycline	2.82×10^{-4}	288.00	0.99926	2.7576	294.24	0.93822

Table S5. The comparison of k_2 (pseudo-second model) and q_e (Langmuir model) on MB, MO and TC adsorption between this study and others from literature.

materials	S_{BET} (m^2 g^{-1})	adsorbate	k_2 (g (mg min)$^{-1}$)	q_{max} (mg g^{-1})	Ref.
Magnetic carbon from mangosteen peels	831.5	Methylene Blue	-	46.296	[2]
Magnetic carbon from corncob	153.89		$3.17x10^{-4}$ at 281.25 mg L^{-1}	163.93	[3]
Magnetite silica gel	597.09		$2.81x10^{3}$ at 250 mg L^{-1}	246.31	[4]
Magnetic graphene sponge	-		$1.5x10^{-4}$ at 175 mg L^{-1}	526	[5]
Amino-functionalized magnetic bacterial cellulose/activated carbon	-	Methyl orange	$1.6x10^{-3}$ at 50 mg L^{-1}	98.33	[6]
Carbon dots/$ZnFe_2O_4$	116.8		$2.7x10^{-2}$ at 20 mg L^{-1}	181.2	[7]
Magnetic chitosan/poly (vinyl alcohol) hydrogel beads	60.1		$2.86x10^{-2}$ at 30 mg L^{-1}	68.86	[8]
Magnetic chicken bone-based biochar	328	Tetracycline	$4.9x10^{-3}$ at 100 mg L^{-1}	63.3	[9]
Chitosan-based magnetic composite particles	8.48		$5.25x10^{5}$ at 100 mg L^{-1}	67.1	[10]
Magnetic carbon composites from bagasse	43.29		$7.52x10^{-4}$ at 80 mg L^{-1}	48.35	[11]
Magnetic carbon adsorbent from water hyacinth	**973.56**	**Methylene blue**	**$9.14x10^{-5}$ at 500 mg L^{-1}**	**524.20**	**This work**
		Methyl orange	**$2.73x10^{-4}$ at 500 mg L^{-1}**	**425.15**	
		Tetracycline	**$2.82x10^{-4}$ at 200 mg L^{-1}**	**294.24**	

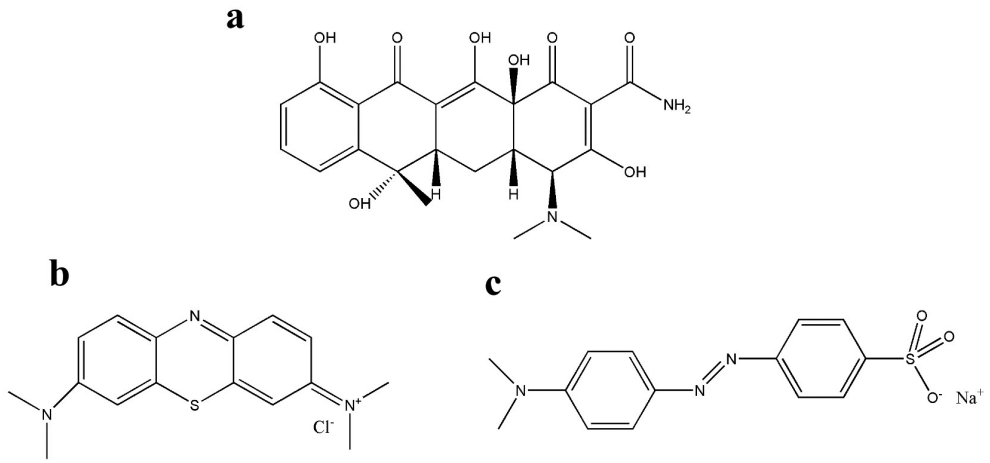

Fig. S5. Chemical structures of adsorbate molecules: (a) TC (b) MB and (c) MO

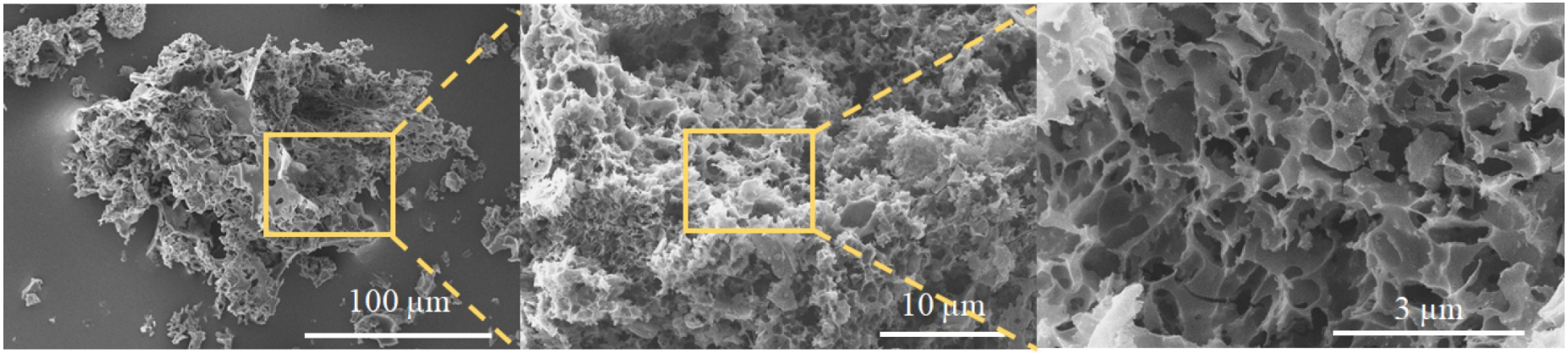

Fig. S6 SEM images of CLP+KOH-800 using different magnifications

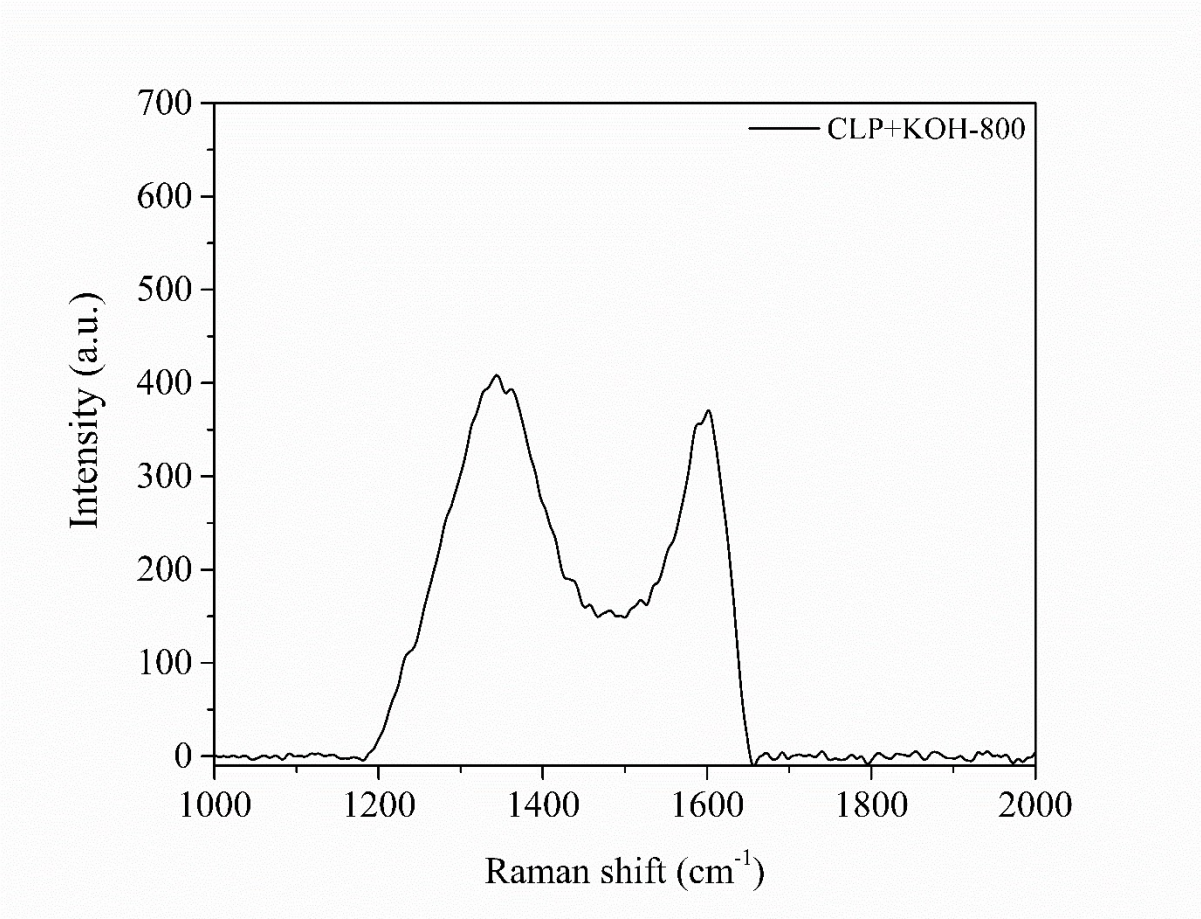

Fig. S7 Raman spectrum of CLP+KOH-800

Equations to calculate capacitance from CVs, GCDs

$$C_{CV} = \frac{4.I}{v.X} \qquad \textit{(eq S1)}$$

$$C_{GCD} = \frac{4.Q}{(\Delta V - IR_{drop}).X} \qquad \textit{(eq S2)}$$

$$C_{EIS} = \frac{4.|Z''(\omega)|}{2\pi\omega(Z'(\omega)^2 + Z''(\omega)^2).X} \qquad \textit{(eq S3)}$$

The following notations are used: I(mA) current, v(mV/s) scan rate of the cyclo-voltammograms, Q(C) the charge accumulated in the porous material calculated during the discharge cycle, ΔV(V) is the voltage window, IR_{drop} (V) is the voltage drop observed when the current is reverse during GCD, ω(Hz) is the frequency, Z'(Ω) and Z"(Ω) the real and imaginary parts of the impedance and X the specific parameter. X is the mass of the working electrode in grams in case of gravimetric capacitance and volume of working electrode in cm^3 in case of volumetric capacitance.

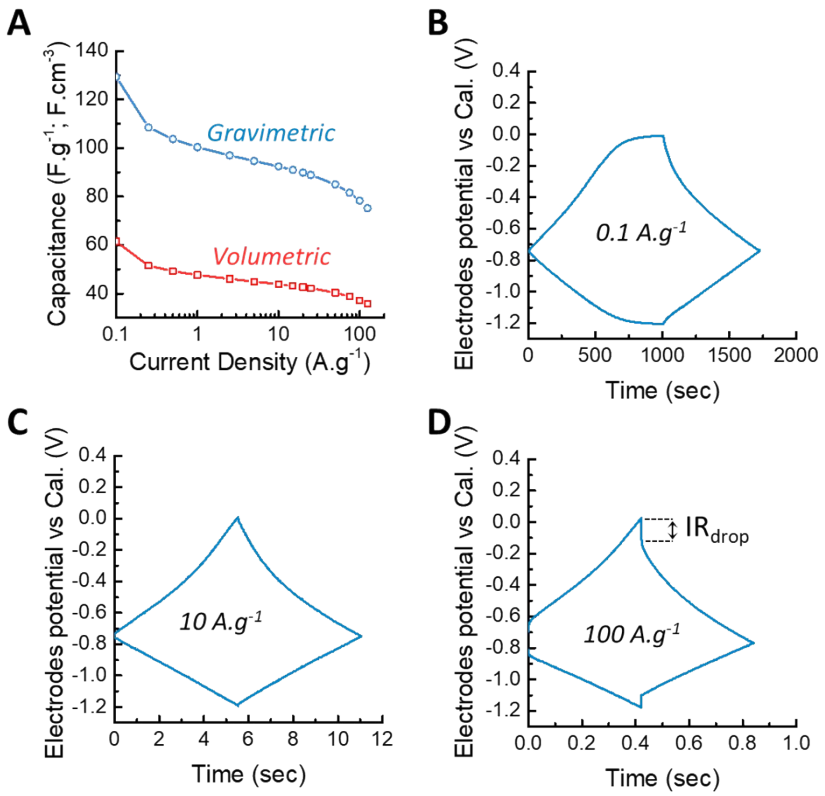

Fig. S8 Electrochemical tests in 6M KOH. (a) Capability of the material calculated from the galvanostatic charge/discharge curves (GCDs); (b,c,d) Simultaneous polarization of the working and the counter electrodes during GCDs at respectively 0.1, 10 and 100 A g^{-1}.

References

1 M. Karthik, E. Redondo, E. Goikolea, V. Roddatis, S. Doppiu and R. Mysyk, *J. Phys. Chem. C*, 2014, **118**, 27715–27720.

2 M. Ruthiraan, E. C. Abdullah, N. M. Mubarak and M. N. Noraini, *J. Environ. Chem. Eng.*, 2017, **5**, 1447–1455.

3 H. Ma, J. B. Li, W. W. Liu, M. Miao, B. J. Cheng and S. W. Zhu, *Bioresour. Technol.*, 2015, **190**, 13–20.

4 S. Z. Guo, H. C. Xu, F. Zhang, X. X. Zhu and X. L. Li, *Colloids Surfaces a-Physicochemical Eng. Asp.*, 2018, **546**, 244–253.

5 B. W. Yu, X. L. Zhang, J. R. Xie, R. H. Wu, X. Y. Liu, H. L. Li, F. Chen, H. Yang, Z. Ming and S. T. Yang, *Appl. Surf. Sci.*, 2015, **351**, 765–771.

6 X. G. Huang, X. Z. Zhan, C. L. Wen, F. Xu and L. J. Luo, *J. Mater. Sci. Technol.*, 2018, **34**, 855–863.

7 W. L. Shi, F. Guo, H. B. Wang, C. G. Liu, Y. J. Fu, S. L. Yuan, H. Huang, Y. Liu and Z. H. Kang, *Appl. Surf. Sci.*, 2018, **433**, 790–797.

8 W. B. Wang, H. X. Zhang, J. F. Shen and M. X. Ye, *Colloids Surfaces a-Physicochemical Eng. Asp.*, 2018, **553**, 672–680.

9 A. A. Oladipo, A. O. Ifebajo, N. Nisar and O. A. Ajayi, *Water Sci. Technol.*, 2017, **76**, 373–385.

10 S. P. Zhang, Y. Y. Dong, Z. Yang, W. B. Yang, J. Q. Wu and C. Dong, *Chem. Eng. J.*, 2016, **304**, 325–334.

11 N. Rattanachueskul, A. Saning, S. Kaowphong, N. Chumha and L. Chuenchom, *Bioresour. Technol.*, 2017, **226**, 164–172.